JOURNAL OF SPACECRAFT AND ROCKETS
Vol. 41, No. 5, September–October 2004

# Effect of Space Environment on Spacecraft Surfaces in Sun-Synchronous Orbits

Jean-François Roussel*
*ONERA, 31055 Toulouse, France*
Irénée Alet† and Delphine Faye‡
*Centre National d'Etudes Spatiales, 31401 Toulouse, France*
and
Alexandre Pereira§
*ONERA, 31055 Toulouse, France*

**Sixteen years of in-orbit measurements of thermal-control coating properties on sun-synchronous SPOT spacecraft are reported and analyzed. Their nonmonotonous evolution is shown to be due mostly to a succession of contamination and contaminant erosion by atomic oxygen phased with the solar cycle. A careful quantitative analysis of the different spacecraft walls and of their time evolution was performed via a semi-empirical model. The major outcome of the model was to indicate the role of the solar UV radiations in enhancing the deposition through chemical bonding. Further UV polymerization of contaminant layers over time was also presumed to be responsible for the decreasing efficiency of the erosion by atomic oxygen.**

## Nomenclature

$C_{\text{sun}}$ = sun constant, around 1340 $\text{W} \cdot \text{m}^{-2}$
$T$ = surface temperature, K
$\alpha_s$ = solar absorptivity
$\varepsilon$ = thermal emissivity
$\sigma$ = Stefan–Boltzmann constant, $5.67 \times 10^{-8}$ $\text{W} \cdot \text{m}^{-2} \cdot \text{K}^{-4}$

## Introduction

THE evolution of the properties of spacecraft surfaces in general and thermal coatings in particular is an important concern because they are degraded in space environments. In-flight evolution of the thermal control properties of the SPOT sun-synchronous spacecraft series has been regularly reported by one of the authors.[1–3] After 16 years of life in orbit, partially encompassing two solar cycles, these data now exhibit enough interesting features to deserve a more detailed physical inspection and a modeling attempt. The analysis reported here aims at determining the physical phenomena responsible for the observed behavior. Despite its limited predictive capabilities, the semi-empirical model presented is thus used to compare different faces of spacecraft and their time evolution to unravel the different physical phenomena involved.

The spacecraft characteristics are presented in next section, which is still quite introductory. The in-flight measurement capabilities and actual measured data are reported in the following two sections, and their analysis is conducted in the subsequent section. A more general discussion follows that precedes the conclusion.

Received 14 March 2003; revision received 16 July 2003; accepted for publication 15 September 2003. 

*Head of Materials, Space Environment Section, Space Environment Department, 2 Av Edouard Belin; roussel@onecert.fr.
†Thermician, Thermal Department, 18 Av Edouard Belin.
‡Chemist, Propulsion, Pyrotechnie, and Contamination Department, 18 Av Edouard Belin; Delphine.Faye@cnes.fr.
§Ph.D. Student, Space Environment Department, 2 Av Edouard Belin.

## French and European Earth Observation Satellites: An Overview

### Missions

SPOT, HELIOS, ERS, ENVISAT, and METOP represent the families of French or European Earth observation satellites. By scanning continents, oceans, and atmosphere, their mission is to study our planet and our environment. They provide a large volume of data for many applications, covering areas such as topographic and relief mapping, meteorology, climatology, agriculture, forestry, geology, land management, military surveillance, telecommunications, and so forth.

### Orbit and Attitude

All these satellites use the same platform derived from the SPOT 1 multimission platform. They are placed in a quite similar orbit, which is circular, ensuring that all the scenes are acquired from virtually the same altitude, about 800 km, there by producing constant resolution and scale. The orbit is also sun-synchronous because the orbital plane must form a constant angle relative to the suns direction to allow similar illumination and thermal conditions and then valid comparison of images of a given location at different dates. In this case, the satellite flies over any given point at the same local time, reaching the ascending nodes approximately at 1030 hrs local time for the SPOT family. Finally, the orbit is phased by choosing a near-polar orbit (inclination 98 deg) to cover the entire planet from north to south, with ready access to any point on the Earth's surface.

The orientation of these satellites is fully controlled relative to three axes. The local orbital reference system is defined by three unit vectors: $\boldsymbol{L}$, collinear to the axis between the Earth's center and the satellite; $\boldsymbol{T}$, perpendicular to the orbital plane; and $\boldsymbol{R}$, which completes the set of orthogonal axes and coincides with the velocity vector. Nominal attitude pointing consists of the best alignment of the satellite axes ($X$, $Y$, $Z$) with the local orbital reference system. Therefore, to accomplish their mission of Earth observation and for perfect geocentric pointing, one face, $Z$, is pointed toward the Earth ($\boldsymbol{L}$) and a second face, $Y$, is directed toward the ram ($\boldsymbol{R}$). Figure 1 shows the orbit configuration.

### Environmental Constraints on Sun-Synchronous Orbit

Such orbits present specific characteristics of the space environment (see, e.g., Ref. 4). First, one orbital revolution is completed in about 100 min. For two-thirds of this orbital period, the satellite is

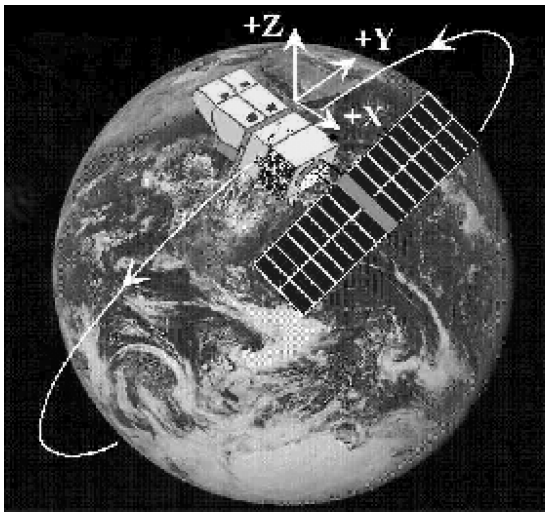


**Fig. 1 SPOT orbit and attitude control.**

in sunshine, whereas for 35 min it is in the Earth's shadow. Therefore, these changes in addition to the external radiation (direct solar flux, albedo, Earth infrared radiation) cause extreme temperature variations on the surfaces of the satellite and then a fast thermal cycling. Besides, in spite of a relatively low altitude (i.e., under the belts of high-energy particles) the satellite can be impacted by electron radiation, especially in the polar regions and in the region of the South Atlantic anomaly. Another important constraint is the density of atomic oxygen, which depends strongly on both the orbital altitude and solar activity. All of these parameters could contribute to modify the thermal balance and affect the aging of external coatings and materials of the satellite.

#### Thermal Control Materials

To maintain the satellite at a moderate temperature for nominal operations, a satisfactory balance must be achieved between heat sources, namely, heat dissipated by electrical and electronic equipment or external electromagnetic radiation, and cold sinks such as deep-space conditions at 3 K. This is why specific surfaces called "radiators" have been designed for use on the outside of the satellite. They are dimensioned to ensure a correct temperature. Their coating is adapted to absorb little solar radiation (small solar absorptance $\alpha_s$) and to emit the maximum of infrared flux (high emissivity $\varepsilon$). This special material, second surface mirror (SSM), is made of a reflective aluminum (Sheldahl G400900) or silver (Sheldahl G404101) metallic surface re-covered by a transparent sheet of FEP Teflon®.

"Superinsulating" blankets or multilayer insulator (MLI) blankets cover surfaces that are not used as radiative areas. They consist of a superposition of about 12 or more thin (7.5-$\mu$m) films of Mylar® with two aluminized faces. The radiative coupling is then very weak. These layers are separated by a fine net of polyester fibers to avoid a conductive coupling. Because the external face is exposed to a space environment, a sheet of polyimide Kapton® (25–50 $\mu$m), a resistant material, has been chosen.

#### Aging of Thermal-Control Coatings

The various space environment factors interact in different ways with space equipment. Their interactions very aggressive toward most materials, particularly for organic ones such as those already cited, and produce a variety of damage. The best known radiation effect is degradation of impinged surfaces. Charged particles (electron, proton, and heavier particles) penetrate into materials and contribute to the breakdown of polymeric chains. The solar UV and extreme UV radiation also critically impact materials by altering external layers and fixing contaminant deposits via polymerization. For instance, a white paint can darken. Atomic oxygen is one of the major constituents of residual atmosphere at low orbital altitude (300 to 800 km). Its large flux can produce dramatic erosion of ram surfaces through oxidation. Thermal cycling of surfaces that go into and out of the Earth's shadow frequently causes stress effects and, hence, an embrittlement of materials. In fact, material degradation depends strongly on synergetic effects of the space environment components.

Different materials age differently through an alteration of their structure and, therefore, their properties, especially their thermooptical characteristics, which are the most important for spacecraft thermal control. Flight experiments have shown that, for a material with a high emissivity, this parameter varies scarcely. On the contrary, the absorptance of radiator coatings (SSM or white paint) increases with aging due to the contamination by outgassed products and material degradation by solar UV and charged-particle radiation. This implies a regular elevation of the mean temperature of the satellite.

## In-Orbit Measurements

#### SPOT 1 and SPOT 2

Eight French or European sun-synchronous satellites have been launched since 1986. The telemetry is regularly analyzed. However, this paper is based on SPOT 1 and SPOT 2 data because these satellites are the first ones of the family and are still operational at the time of this writing. Their duration in orbit is, respectively, 16 and 12 years. (SPOT 1 was launched on 22 February 1986 and SPOT 2 on 22 January 1990). On each platform, 50 temperature measurements are performed every 16 s. The temperature of the radiators located on four faces of the satellite will be studied ($+Y$, $-Y$, $+Z$, $-Z$, i.e., trailing, leading, zenith, and nadir faces, respectively).

#### THERME Experiment

When the first SPOT satellite was developed, there was an important lack of information about aging of materials in sun-synchronous orbit. In fact, until the 1980s, experimental efforts had mostly been directed toward materials in geostationary orbit. This is why THERME, a simple and low-cost experiment, was designed and boarded on SPOT 2, 3, 4, and, in the near future, will be used on six other satellites: SPOT 5, HELIOS II (2 experiments), STENTOR, FBM, and DEMETER.

The principle of THERME is to measure the in-orbit temperature of a material during the sunlit phase. Supposing that the variation of the infrared emissivity is weak enough to be neglected, the solar absorptance can be easily deduced from the telemetry.

A THERME sensor consists of a small sample (100 × 100 mm) of a given material to test with a thermistor placed on the back face as shown in Fig. 2. It is fixed on the external side of an MLI blanket and exposed to the space environment on the front side of the satellite (to receive a large flux of atomic oxygen) and on the other sides when area is available. Figure 3 shows four THERME sensors placed on SPOT 4. The experiment has the advantage of not consuming electrical power. The only constraint for the satellite is a temperature measurement every minute.

## Observations

#### In-Orbit Evolution of Temperatures

Figures 4 and 5 present the time evolution of temperatures for the walls of SPOT 1 (over 16 years) and SPOT 2 (over 12 years),

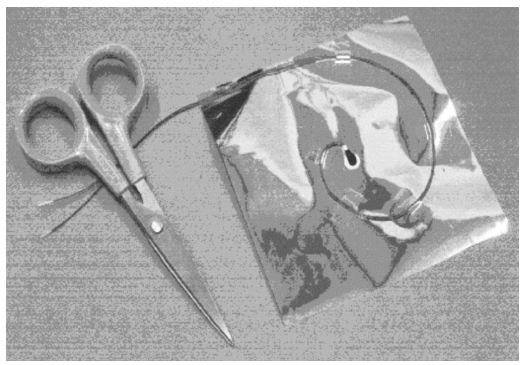

**Fig. 2 Thermistor on the back face of a THERME sensor.**

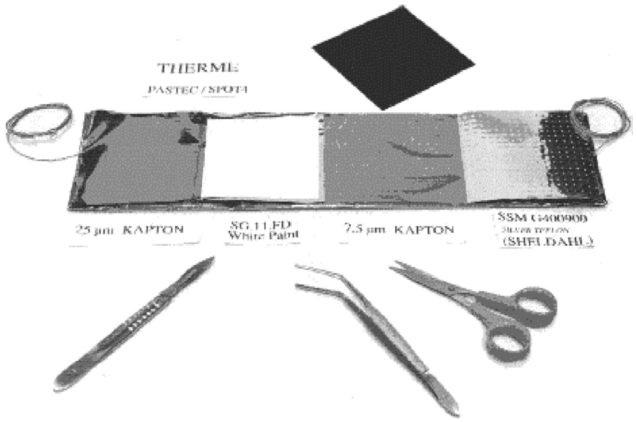


**Fig. 3 Example of four THERME sensors placed on SPOT 4.**

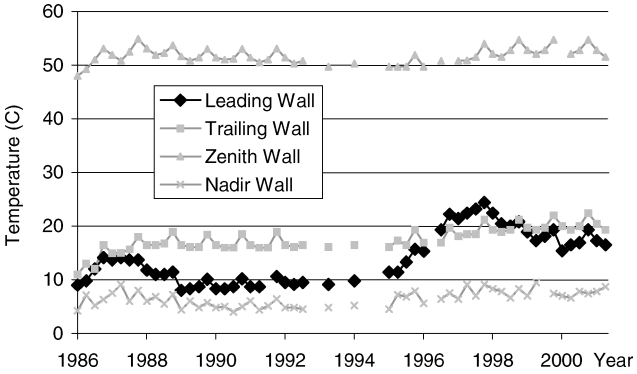


**Fig. 4 Time evolution of temperatures of four walls of SPOT 1.**

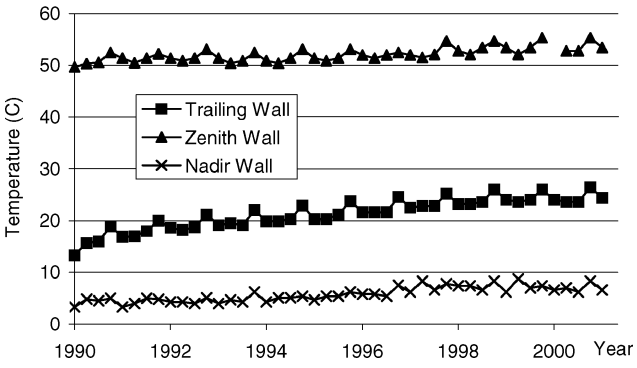


**Fig. 5 Time evolution of temperatures of three walls of SPOT 2.**

respectively. Figure 6 presents the time evolution of four THERME experiments on SPOT 2, two of them based on SSM–Teflon and two on SSM–Kapton.

### In-Orbit Evolution of Solar Absorptance

Assuming no emissivity change, temperature changes have been translated in terms of solar absorptance variation of the walls of SPOT 1 and SPOT 2 in Figs. 7 and 8. The solar absorptance variation of four THERME experiments on SPOT 2 is displayed in Fig. 9. The solar absorptance initial value for the aluminum SSM (G400800 from Sheldahl) was measured to be 0.15. It covers leading, trailing, and Earth walls of SPOT 1 and 2, and half of THERME experiments. It was 0.33 for the Kapton-based THERME experiments. In all cases the infrared emissivity $\varepsilon$ was assumed unchanged, because material aging is known to generally mostly affect solar absorptance, at least much more than emissivity. The same is true for the contamination of thermal coatings because contaminants have an emissivity similar to coatings (large) and a much larger absorptivity. Another effect could yet significantly change the emissivity of

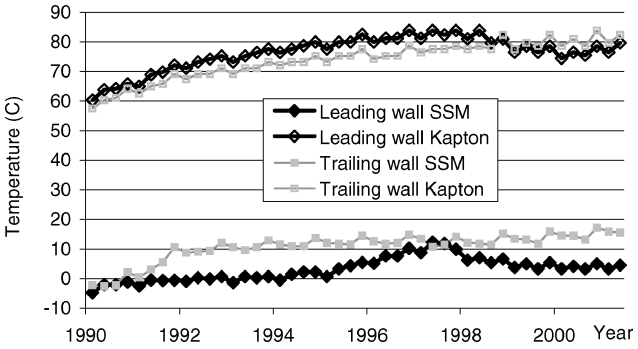


**Fig. 6 Time evolution of temperatures of four THERME experiments on SPOT 2.**

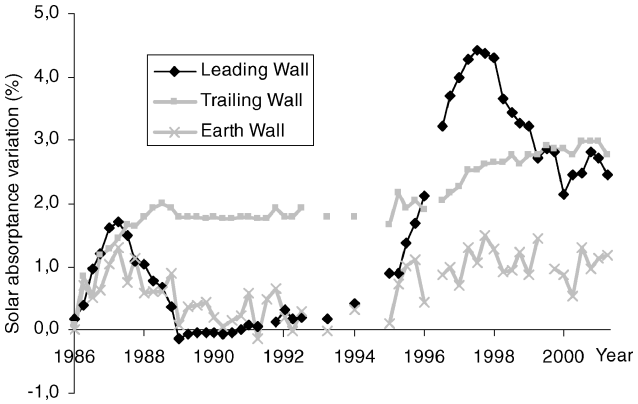


**Fig. 7 Time evolution of solar absorptance of three walls of SPOT 1 ($\Delta\alpha_s = 1\%$ means $\Delta\alpha_s = 0.01$) covered with aluminized SSM–Teflon (Sheldahl G400800); initial absorptance is 0.15, initial emissivity is 0.78, assumed unchanged.**

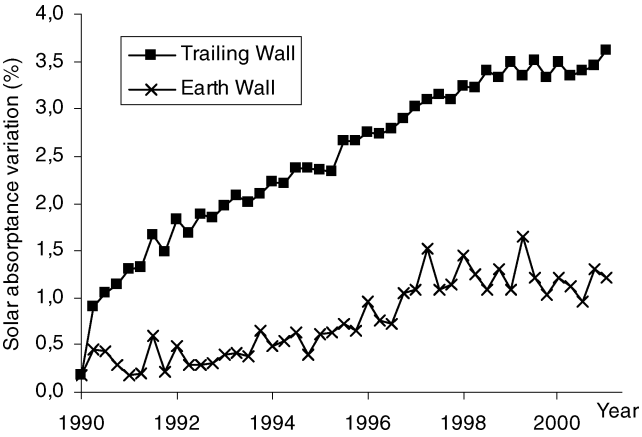


**Fig. 8 Time evolution of solar absorptance of two walls of SPOT 2; similar material properties as for SPOT 1 (cf. Fig. 7).**

Kapton: the reduction of its thickness via erosion by atomic oxygen (AO). However, the erosion was assessed to be 3 $\mu$m over one solar cycle, which should result in an $\varepsilon$ decrease of 0.015. This effect was considered small enough to consider Kapton emissivity constant to keep homogeneous presentation of the results. We must yet be aware that it results in an erroneous interpretation as a 0.01 increase of Kapton solar absorptance (denoted $+1\%$), which remains an acceptable inaccuracy when compared to typical $\Delta\alpha_s$ on the order of 10% (so, after 12 years in orbit the leading-wall Kapton $\alpha_s$ is indeed 1% lower than represented on the second curve of Fig. 9).

Note that the solar absorptance variations are given here in absolute percentage, not relative: $\Delta\alpha_s = 1\%$ means $\alpha_s \to \alpha_s + 0.01$, not $\alpha_s \to \alpha_s + 0.01 \times \alpha_s$.

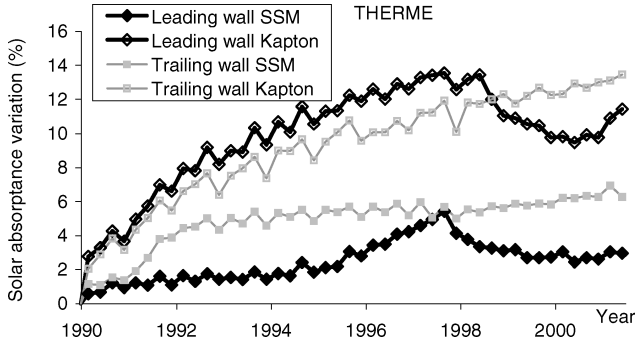


**Fig. 9 Time evolution of solar absorptance of four THERME experiments on SPOT 2. Aluminum/SSM–Teflon and 25-$\mu$m Kapton have initial absorptances of 0.15 and 0.33, respectively; their emissivities are 0.78 and 0.63 and are assumed unchanged for simplicity. (This assumption results in a 1% overestimation of leading-wall Kapton absorptivity $\alpha_s$ after one solar cycle, indeed due to an emissivity decrease of 0.015 because of AO erosion.)**

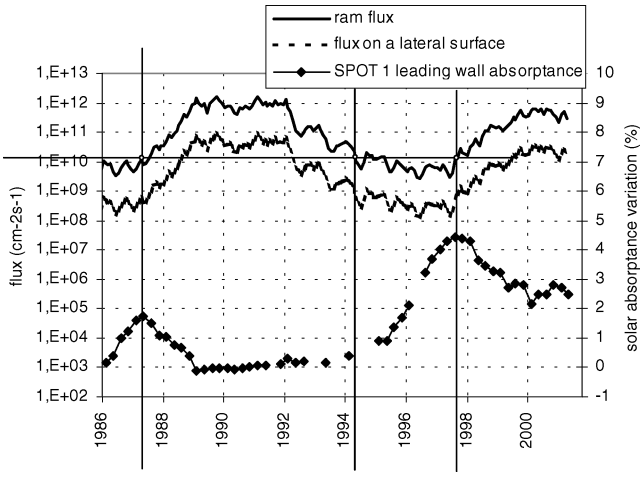


**Fig. 10 AO fluxes on SPOT orbit and leading-wall absorptance variations are consistent with a threshold around $1.5 \times 10^{10}$ $O^+ \cdot cm^{-2} \cdot s-1$ (degradation below the threshold, erosion and cleaning above).**

The translation of temperature data in Figs. 4–6 into the absorptivity changes of Figs. 7–9 indeed relies on a thermal model. The THERME experiments were designed to be insulated from the spacecraft, on top of the MLIs. The thermal exchanges are thus reduced to radiation transfers and thermal analysis simply yields

$$d\alpha_s = \frac{4\varepsilon\sigma T^3}{C_{\text{sun}}}\, dT \tag{1}$$

where $\sigma$ is the Stefan–Boltzmann constant and $C_{\text{sun}}$ is the sun constant. A small correction was added to account for the small seasonal variations of the sun constant and of the small heat conduction through the MLIs. The case of the temperature of the spacecraft walls is more complex and would require a full thermal model of the spacecraft to take into account the variations of conductive transfer to the walls. In the absence of knowledge of the variations of absorptivity on other surfaces (and other thermal parameters) this task looked unfeasible, or at least beyond available time resources for this study. An approximate analysis was thus conducted, which led to the values shown in Figs. 7 and 8. Considering that the global heat rejection is constant (constant power used onboard), the conductive transfer change is only due to a change in the rejection distribution between radiator walls. We thought that the temperature change of a wall could reasonably be considered predominantly affected more by its own absorptivity change than by the conduction to another wall of modified absorptivity. Thus, considering the changes of conductive transfers small compared to the changes of sun radiation absorption led to Eq. (1) for the walls also. The use of Eq. (1) in this case also may yet have resulted in some quantitative errors, such as influence of one wall on another wall through conduction, but we considered that they were reasonable compared to other parameter uncertainties of the forthcoming model and did not change the physical interpretation of the data.

This law, Eq. (1), is however not true for the zenith wall coated with golded Kapton. There, the increase in solar absorptance is not significantly compensated by thermal emission because of the small emissivity of gold ($\varepsilon = 0.03$ to 0.04). In this case the dominant compensation effect is the increase of the conductive heat flux to the spacecraft. Due to the difficulty of estimation, these zenith data were simply excluded from the forthcoming analysis (as can be seen in Figs. 7 and 8).

## Interpretation

### Qualitative Analysis

A fundamentally different behavior is observed between the leading face and the other faces, especially the trailing face. Indeed, the trailing face ages regularly and becomes slowly warmer because of the regular increase of solar absorptance. On the contrary, the evolution of the leading face is cyclic with high aging periods followed by a return to quasi-initial temperatures. This unexpected thermal behavior has been observed on SPOT 1 since 1989 and thereafter on all of the other satellites in sun-synchronous orbit; this phenomenon has been better investigated. In fact, all environmental parameters could affect the aging of external coatings and materials and modify the thermal equilibrium. However, these effects are almost the same for any face; the only difference is the exposition to AO flux: the leading face, is the most exposed face, whereas the flux is small or negligible for the other faces. Nevertheless, before these observations, we thought that AO effects were not significant at such high altitude (820 km). The telemetry analysis over long periods has proved the contrary.

Moreover, the cyclic evolution of temperature of the leading face of these satellites is synchronized with the cyclic solar activity, which notably influences the AO density, as shown in Fig. 10. This is the second proof that there is a link between this behavior and the AO effects that can counterbalance the effects of material aging or of the contamination by eroding the deposits. More precisely, Fig. 10 shows that the succession of degradation and curing periods for the SPOT 1 leading wall is consistent with a threshold for the AO flux on the order of 1 to $2 \times 10^{10} O \cdot cm^{-2} \cdot s^{-1}$. Smaller fluxes allow contamination buildup, whereas larger fluxes erode deposited contaminants.

If we considered the aging of the other faces, the same phenomenon as in the ram direction is indeed also observed but with a smaller amplitude. The lateral zenith and Earth faces, parallel to the velocity vector, receive AO because of the thermal velocity of these atoms. The trailing face should not receive AO because of the large gap between the satellite velocity and the thermal motion velocity. However, there is a tiny effect, shown in Figs. 4–6, which requires some explanation and will be discussed in subsequent text.

### First Quantitative Analysis

Before trying to build a real model accounting for these data in next section, a more quantitative analysis of these absorptance evolutions can be performed. Periods of degradation and curing show up alternatively following the solar cycle.

Let us first consider the degradations during solar minima. During the first solar minimum in 1986, only SPOT 1 had been launched and was spending its first year in orbit. All its surfaces degraded quite similarly, with an approximate degrading rate of 1%/year for $\alpha_s$. This is consistent with a beginning-of-life contamination due to higher initial outgassing rates of materials. During the second minimum in 1995–1997, most surfaces exhibited a greatly reduced degradation rate in the range of 0.2 to 0.4%/year. This is consistent with a decrease of the outgassing after 9 and 5 years in orbit, respectively, for SPOT 1 and SPOT 2. However, the leading walls continue to degrade at 1%/year or more. This quick degradation for ram-facing walls after a long time in orbit is very clear in Figs. 4 and 7. It can only be explained by the photoenhanced contamination

due to the specificity of sun-synchronous orbit (leading wall is always sunlit at eclipse exit), which will be discussed later in the text.

Two recovery periods are visible during solar maxima, in 1988–1993 and 1998 until the present. The ram-facing surfaces always experience recovery rates close to 1%/year, whether at the beginning or end of life. Surfaces impinged at grazing incidence by the residual atmosphere (zenith and Earth) experience a reduced recovery (0.3 to 0.4%/year at beginning of life of SPOT 1) or simply a stop of the degradation (end of life of SPOT 1 and SPOT 2). This is qualitatively consistent with the reduction of the flux onto such surfaces; that grazing flux is due to thermal dispersion and should be around 5% of the ram flux. The contaminant erosion is certainly more difficult at the end of life than at the beginning of life because contaminants had more time to be UV-polymerized, which explains the degradation stop instead of a recovery. The same feature is visible in the extent of the recovery. Whereas the recovery is almost complete at the beginning of life (SPOT 1, leading and nadir walls at least), it is only partial at the end of life (2% recovery vs 4% degradation for SPOT 1 leading wall). This might indicate that even the larger ram AO flux is insufficient to erode the whole contaminant layer after several years of UV exposure and reticulation. This incomplete recovery could also be due to silicone contaminants oxidized into $SiO_x$, although there is no evidence of their presence in the data before 1999. It is unlikely to be caused by intrinsic material degradation because the net degradation after partial recovery (+2% between 1994 and 2000 for SPOT 1 leading wall) is much larger than the continuous degradation observed during the previous years +0.5% between 1989 and 1994; see Fig. 7), which is certainly due to material degradation.

Trailing walls also seem to experience a stop of the degradation during solar maxima (SPOT1, SPOT2) if not a small curing (SPOT 1). That small effect of AO density increase on the wake-facing surfaces may be due to ionized oxygen ions ($O^+$) that have the capability to be attracted into surfaces in the wake as soon as such surfaces charge a few volts negative. Although not well characterized, the efficiency of erosion by $O^+$ ions is likely to be larger than the one by neutral AO, which could somewhat compensate for the smaller flux of $O^+$ onto such surfaces. The average $O^+$ flux is of the order of $10^{10} O^+ \cdot cm^{-2} \cdot s^{-1}$ on SPOT leading walls and is less dependent on solar cycle than the AO flux. It gives an $O^+/O$ ratio in the percent to tens of percent range on ram faces but is unknown for wake faces.

## Modeling

### Methodology

The quantitative features of thermal-control degradation were exhibited and analyzed as accurately as possible. Some physical processes were identified: contaminant deposition, cleaning by AO, and maybe UV enhancement of the deposition on some surfaces, discussion of which will be postponed to next section. The next step of this analysis consists of building a quantitative model of these phenomena.

The standard procedure for assessing thermal-control coating degradation would be to characterize the contaminant sources on SPOT and compute their transport, deposition, and effects on materials. Intrinsic material degradation should also be accounted for based on our best knowledge of environment material interactions. Unfortunately most of these processes cannot be assessed with an accuracy better than, typically, a factor of 2. The global accuracy of the absorptance variation predictions would even be much worse than that, because phenomena even more poorly characterized are involved. such as contaminant erosion by AO and UV fixation. The flight data could thus very easily fall inside the huge error bars but no interesting lesson could be learned from the comparison.

It was thus decided to use a reverse methodology. Empirical reasonable laws involving free parameters were written for each phenomenon involved: deposition, erosion, and effect of contaminants, and also the intrinsic degradation of bulk material. These parameters were then fitted to yield absorptance variations as close as possible to the flight data. The values obtained by this method are not considered as very accurate but rather as a basis for a physical analysis in the next section (Discussion and Lessons Learned).

We must insist that fitting data with empirical laws involving free parameters is a very risky strategy. It is very easy to add enough parameters to fit the data correctly and still be far away from any correct physical interpretation. Several rules were thus followed to avoid such a misleading attitude:

1) Consider as few parameters as possible.

2) Always check that there are much more data than free parameters.

3) Check that the optimal values found for the parameters make sense physically.

4) Replace a free parameter with a fixed value as soon as possible.

### Model

The parametric laws in use were the following. The variation $\Delta\alpha_s$ of the solar absorptance $\alpha_s$ due to aging of the intrinsic material was modeled as a power law:

$$\Delta\alpha_s = Dt^a$$

where $\Delta\alpha_s$ is measured in percent and $t$ is measured in years. There should be a different pair of parameters $D$ and $a$ for each different material but not for each face because almost all spacecraft faces considered have the same UV fluxes: 2000 to 2600 equivalent sun hours (ESH)/year for leading, trailing, and zenith faces and only 350 ESH/year for the nadir face. Radiation fluxes are also comparable, because the high-energy particle fluxes are not too far from isotropic. (Again, a lower dose for precipitating electrons onto the nadir face may be expected.)

The model of contaminant deposit thickness has two components: a linear cumulative contribution (constant deposit) typical, for example, of constant contaminant sources (thrusters, degradation of materials), and a power-law cumulative contribution $C\sqrt{t}$ (hence, outgassing in $1/\sqrt{t}$) more typical of outgassing. There should be a different set of parameters for each different face, but not for different substrates, because contamination deposition was considered substrate independent, which is reasonable from the second deposited layer.

The next law characterizes the change of solar absorptance due to the typical contaminants on the SPOT spacecraft series. Most contaminants are indeed only optically active after UV irradiation (UV darkening) and the time-dependent darkening process should in principle be modeled. However, typical time scales for UV darkening (a few thousand of UV ESH) are relatively small compared to the observation time scales (a few years, hence many thousands of ESH). Moreover, we wanted to avoid introducing extra parameters as much as possible, in accordance with the methodology described earlier. Therefore, we simplified the model by considering that the darkening is immediate and happens at contaminant deposit. For the small deposits involved, the darkening law is certainly a linear function of the thickness and simplifies into a single coefficient. A widespread typical value is 1% of $\alpha_s$ increase for 100 Å deposited (after UV darkening). Experiments at the ONERA Space Environment Department showed around 1.3% of $\alpha_s$ increase per 100 Å of silicone deposited on an optical solar reflector. A value of $\Delta\alpha_s = 2.5\%$ per 100 Å deposited was also reported for polydimethylsiloxane deposited on the SSM.[5] These values are obtained after a UV exposure equivalent to less than one year in low Earth orbit (LEO) (except for nadir surfaces), which is consistent with the aforementioned immediate UV darkening hypothesis. This coefficient is considered identical on every surface and spacecraft (same type of contaminants assumed) and was indeed fixed to 1%/100 Å.

A final law is needed to characterize the contaminant erosion by AO. It is assumed linear and the yield was considered relatively to the Kapton erosion yield by AO ($3 \times 10^{-24}$ cm$^3$/atom). Contaminants physically adsorbed and then chemically fixed through some partial cross-linking can reasonably be thought of as more easily eroded than Kapton (except for silicones transformed into $SiO_x$). Hence, this coefficient could be assumed somewhat larger than 1, but it is mostly unknown. Here again it is assumed identical on every surface and spacecraft. Contaminant erosion is thus only modulated by the fluxes of AO onto the surfaces, through their orientation with respect to ram, and through the AO ambient density.

**Table 1 Parameters used for empirical modeling of solar absorptance evolution**

| Face | Contamination: Deposition, linear law | Contamination: Deposition, $C$ constant in $C\sqrt{t}$ law | Contamination: Erosion by AO | Contamination: Effect on $\alpha_s$ | Intrinsic degradation of SSM–Teflon |
|---|---|---|---|---|---|
| Leading | 70 Å/yr | 0 | 3 times more than Kapton | 1% of $\alpha_s$ increase per 100 Å deposited | 0.1 $t$ |
| Nadir | 0 | 40 Å the first year | 3 times more than Kapton | 1% of $\alpha_s$ increase per 100 Å deposited | 0.06 $t$ |
| Trailing | 0 | 70 Å the first year | ——[a] | 1% of $\alpha_s$ increase per 100 Å deposited | 0.1 $t$ |

[a]Different AO erosion yields were used for old and newly deposited contaminants, 2 and 20 times the Kapton, respectively.

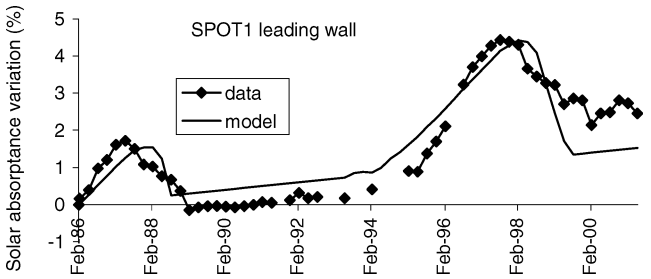


**Fig. 11 Solar absorptance of SPOT1 leading wall: comparison of flight data and model.**

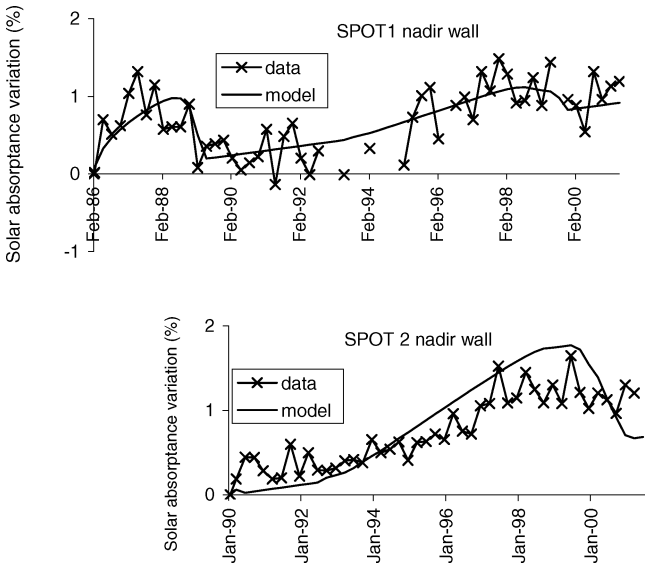


**Fig. 12 Solar absorptance of SPOT1 and SPOT 2 nadir wall: model parameters adjusted to fit SPOT 1 data and then used for SPOT 2.**

**Comparison to Leading- and Nadir-Wall Data**

The leading, nadir, and zenith walls receive the largest AO fluxes and thus exhibit the most characteristic and easiest-to-interpret features; the analysis should thus begin with them. The model parameters that allow the best fit of these experimental data are given in Table 1. The comparison of the model and the flight data is displayed on Figs. 11 and 12. When data were available both for SPOT 1 and SPOT 2, the parameters were first optimized to fit SPOT 1 data and then applied to SPOT 2 (nadir wall; Fig. 12).

The fit of SPOT 1 leading-wall data displayed in Fig. 11 is satisfying. It required the assumption of a constant contaminant deposition rate (70 Å/year) to account for the large degradation after 10 years in orbit for SPOT 1. The linear intrinsic degradation of its SSM–Teflon coating ($\Delta\alpha_s = 0.1t$) accounted correctly for the small linear degradation during the solar maximum of 1989–1992. The solar absorptance after the first recovery during the first solar maximum (around 1988) is lower than the initial one. It may be due to some preflight contamination that was cleaned by AO. The second recovery (around 1999) was partial and is certainly due to

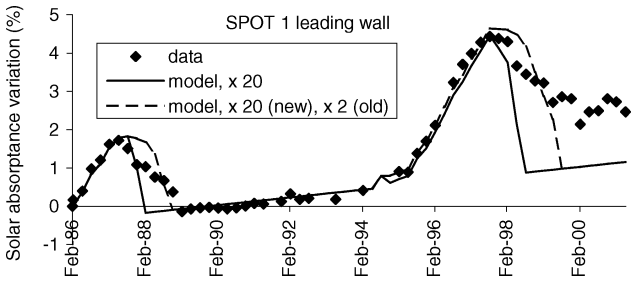


**Fig. 13 Different modeling of SPOT 1 leading wall: higher efficiency for AO erosion (20 × Kapton), higher efficiency for new contaminant and lower efficiency (2 × Kapton) for old contaminant deposited years before. (In both cases contamination was increased to 175 Å/year and an initial contamination of 25 Å was assumed.)**

some highly reticulated contaminants after several years of exposure to the space environment, or maybe to silicones, as discussed in the preceding section. The model does not take these two extra phenomena into account; this is why the model underestimated the 1988 recovery and overestimated the 1999 recovery.

SPOT 1 nadir-wall data were correctly modeled (Fig. 12) through a decreasing contamination rate (cumulated contaminant $40\text{Å} \times \sqrt{t}$) accounting first for an important degradation (and total recovery) and second for a slower degradation. The data were again consistent with a linear intrinsic degradation of the SSM–Teflon coating but with a smaller amplitude ($\Delta\alpha_s = 0.06t$). The modeling of SPOT 2 nadir-wall evolution with parameters optimized for the SPOT 1 nadir wall was globally satisfying, which proves this empirical model has some predictive character (for the same type of spacecraft). However, it yielded an important recovery in 1999–2000, whereas flight data only exhibit a halt in the degradation. This is again certainly due to the increased difficulty for AO to erode contaminants deposited much earlier.

When comparing all of these data and models, another general discrepancy between the models and the data shows up. In the models, the degradation is slower, starts earlier, and stops later than in the data (clear on SPOT 1 leading wall). On the contrary, the recovery is faster and more complete in the model (visible in almost all data). This last observation (only partial recovery on the data in 1999–2000 after many years in orbit) was already stated and interpreted as originating from the lower efficiency of AO erosion on highly polymerized/reticulated contaminants. The other features (too-slow degradation and too-fast curing in the model) are certainly due to the same kind of mechanism.

We tried to implement this idea in the model by assuming a higher erosion efficiency of the contaminants just deposited, which also forced us to consider a larger contamination rate. This effectively led to later and faster degradation. Figure 13 shows, for instance, that considering contamination erosion 20 times more efficient than Kapton gives the right degradation slope and timing. (Meanwhile, the contamination rate had to be increased from 70 to 175 Å/year). A second attempt to improve the fit is reported in the second curve of Fig. 13. In contrast to the easy erosion of newly deposited contaminants, the erosion of old polymerized contaminant was considered only twice efficient as Kapton. The model shows that this assumption delays the recovery. Although delayed, the recovery does not have the right shape; in the model the recovery speed increases with

the increasing solar cycle (concave model curve in 1988 and 1998–1999), whereas the actual recovery rate decreases (rather convex data curve in 1988 and 1998–1999). There looks to be only one possible physical explanation for the decrease of the erosion rate while AO flux is increasing. When erosion reaches deeper contaminant layers, they are more and more difficult to erode because they have spent more and more time exposed to the space environment until eventually the erosion reaches layers that cannot be eroded by the maximum flux of the years 2000–2001, which results in the stationary condition of 2000–2001. This is not an unreasonable explanation because assuming an erosion yield as low as typically one-tenth of the Kapton yield (a few $10^{-25}$ cm$^3$/atom) is enough to make erosion negligible during that solar maximum. This yield is not smaller than the yield of Teflon erosion by AO, in the range of 0.4 to 8 $\times$ to $10^{-25}$ cm$^3$/atom, depending on measurements and synergies.[5,6] It does not look unreasonable for highly reticulated contaminants, where some of them are possibly fluorinated. It makes this explanation more likely than a silicone contamination, which indeed would not be very consistent with the absence of incurable contamination on SPOT 1 at the beginning of its life.

A global look at the intrinsic degradation laws that were found to best fit the data is also in order. The intrinsic degradation of Teflon is small on the SPOT sun-synchronous orbit at 825 km. It is thus in the initial linear part of the classical degradation curve of materials in space, far from the saturation. This is why a linear law was chosen for SSM–Teflon, and indeed it turned out to fit better the data than, for instance, a square-root-of-time law such as the one used for Kapton. A good fit of flight data was obtained with a coefficient of 0.1%/year for $\alpha_s$ degradation on leading (and trailing) walls and 0.06%/year for nadir walls. These values are consistent with the 3%/year observed in (quasi-) geosynchronous Earth orbit (GEO) on SCATHA[7] reduced by a factor of almost 100, typical of the ratio of ionizing radiations between GEO and the 825-km sun-synchronous orbit of SPOT. The degradation is smaller on nadir surface most likely because the largely reduced UV flux does not enhance the radiation-induced degradation, contrary to other surfaces.

#### Comparison to Other Data

The behavior of the trailing walls was more difficult to explain. The monotonously increasing absorptance of the SPOT 2 trailing wall (Fig. 8) could simply be understood as a monotonous buildup of contamination that could not be eroded by the AO, which was unable to reach that wake-oriented surface (although a halt in degradation can be seen in 1999–2000); but the SPOT 1 trailing wall exhibited small recoveries during solar maxima, or at least a very clear halt of degradation (Fig. 7). The synchronization with solar cycle again indicates AO erosion. A few oxygen atoms or, more probably, ions attracted by small negative potentials are certainly able to reach this surface.

Even when assuming a nonzero AO flux onto these trailing walls, another puzzling feature was hard to understand. The SPOT 1 trailing-wall degradation stops in September 1988, about six months before the maximum of AO flux is reached around March 1989. If the September 1988 flux ($2.4 \times 10^{11}$ cm$^{-2}$s$^{-1}$) is enough to stop contamination, the much larger flux of March 1989 and later (around $1 \times 10^{12}$ cm$^{-2}$ s$^{-1}$) should cause a contamination decrease. This puzzling phenomenon might be explained by an improbable inaccuracy of the AO flux model (mass spectrometer incoherent scatter). But, even then, it would be really surprising to have had exactly the correct AO flux during the 1989–1990 maximum to just prevent contamination but not erode previous contaminant layers and get a recovery. The only reasonable and natural explanation is again the one discussed at the end of previous section, which allowed great improvement of the accuracy of SPOT 1 leading-wall modeling. The erosion of newly deposited contaminants (not yet highly polymerized, maybe only physically adsorbed) must be much easier than the erosion of contaminants deposited a long time ago and highly UV-polymerized. Again, using the values that allowed for a correct fit of SPOT 1 leading-wall data (erosion 20 and 2 times more efficient than Kapton's, respectively) gives a good fit of the data, as shown in Fig. 14.

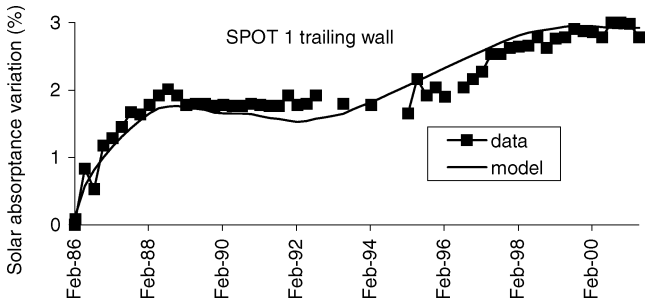


**Fig. 14 Model of SPOT 1 trailing wall with higher erosion efficiency for new contaminant (20 × Kapton) and lower efficiency for old contaminant (2 × Kapton) (cumulated deposited contaminant assumed $70\sqrt{t}$ Å, time $t$ in years).**

The trailing wall of SPOT 2 exhibits a slightly larger degradation than on SPOT 1 (3.5% in 12 years instead of 3% in 16 years). Its behavior can be reproduced by invoking the same phenomena as just discussed for SPOT 1 with slightly different parameters.

We might also wonder whether the curing or degradation halt observed on trailing walls could not originate in the small thermal coupling existing with other walls, which was neglected in the preceding thermal analysis. The curing and cooling of other walls would be the source of the cooling of the trailing wall. However, this phenomenon happens significantly later on the trailing wall than on the other walls (one year later or more; see Fig. 7 for a clear delay on SPOT 1). This delay is not consistent with a thermal coupling, which would have immediate effects. On the contrary, it is consistent with the need for a larger flux to cure the trailing faces. The AO fluxes in Fig. 10 show that the threshold flux for a degradation halt in late 1988 and 2000 would be on the order of a few $10^{11}$ $O^+ \cdot cm^{-2} \cdot s^{-1}$ for the ram flux. When comparing this value to the $1.5 \times 10^{10}$ $O^+ \cdot cm^{-2} \cdot s^{-1}$ threshold for leading-wall curing, we can either conclude that the AO flux on the trailing face of SPOT is only reduced by a factor of 20 to 50 with respect to the ram flux or invoke larger $O^+$ effects in the wake.

The final data to examine are from THERME experiments. The degradation levels are larger than on SPOT 1 or 2 walls. In the case of Kapton coatings, it is of course due to the degradation of the Kapton absorptance, which is much larger than the Teflon absorptance. But THERME experiments coated with SSM–Teflon also experience a larger degradation than the SSM-coated walls. The most probable explanation is related to the different thermal behavior of the big spacecraft walls and the small THERME experiments. The latter have smaller thermal inertia and experience deeper thermal cycles. They can thus condense more contaminants, which leads to a larger amount of polymerized contaminants stuck for the long term. The data are consistent with contaminant deposition rates somewhat larger than on the walls and with a degradation of Kapton on the order of $\Delta\alpha_s = 3 \times t^{0.4}$% ($t$ in years), although it is not very easy to separate contamination from degradation on so few data. The data fits are not reproduced for lack of space, just as for the SPOT 2 trailing wall.

## Discussion and Lessons Learned

After a physical examination of the flight data, a simple empirical model of the degradations and recoveries of the thermal coatings was developed. All available data were modeled and the optimal parameters were determined for contamination, erosion by AO, and material intrinsic degradation.

#### Contaminant Deposition Rates

Looking back at all the contamination deposit laws that were found to best fit the data, a striking feature shows up. Most data were found consistent with a classical time-decreasing deposition rate, with a typical law for cumulated deposit thickness $50\sqrt{t}$(Å) ($t$ in years). But the leading walls are rather consistent with a constant deposition rate, typically $70t$ Å (see Table 1). Not only is the behavior different, but the cumulated amount over 12 or 16 years is

also much larger on leading walls (by a factor of 5). Although an accurate assessment of the contaminant sources on all surfaces was not performed for lack of data, all surfaces are thought to be quite similar. Moreover, a constant deposition rate is inconsistent with any outgassing law, which is always time decreasing. No significant thruster firings are performed on the trailing wall either. This large constant deposit rate was thus rather puzzling, until we realized a specificity of SPOT sun-synchronous orbit: the leading wall is always directly sunlit at eclipse exit, contrary to zenith, nadir, and trailing surfaces.

The fixation of contaminants by the sun UV photons explains all of these features. First, photodeposition is obviously more important on the leading wall. Contaminants get condensed during eclipse on top of the thermal coatings. At eclipse exit these contaminants are reevaporated while these coatings heat up due to the direct sun exposure or to the global spacecraft heating. Therefore, only the surfaces that are exposed to the sun during that heating period following eclipse exit can have their contaminants chemically bonded by energetic UV. In the SPOT sun-synchronous orbit, such is the case for the leading wall only (and also for a lateral wall not considered here). UV-enhanced deposition is thus the explanation for the larger deposition rate of the leading wall.

Second, the different time dependence of the leading-wall deposition rate, namely, a rather constant rate, is typical of photoenhanced deposition. Such a flat time dependence was observed, for instance, on the global positioning system[8] and explained by photodeposition, which becomes photolimited when the contaminant flux is large compared to the capability of the vacuum ultraviolet flux to fix it.[8,9] Even though these results were obtained for geostationary steady-state conditions very different from the fast thermal cycling of LEO, a similar behavior could be expected for UV-enhanced deposition on SPOT. Extra work has begun on this subject.

An alternative explanation of the constant contaminant deposition rate on ram-facing surfaces could be that contaminants originate from (constant) material degradation and not from outgassing. For instance, material erosion by AO produces molecular fragments on the leading wall only, which can be redeposited and UV fixed. But these AO erosion products can be eroded again by AO or, stated differently, contamination builds up only when AO flux is small (1986, 1995–1997), which is inconsistent with contaminants originating from AO erosion. (AO erosion is then only a few angstroms per year.)

#### Erosion by AO

Thorough analysis of flight data revealed very interesting features for contaminant erosion by AO. First, several sets of data could be fitted much better if a higher erosion yield is assumed for contaminants just adsorbed than for layers deposited some time ago (SPOT 1 leading and trailing walls on Figs. 13 and 14). Second, the first layers deposited a shorter time ago looked easier to erode than the deeper layers deposed earlier. The present simple model considers the total contaminant deposit globally and could not account for this multilayer effect. Although not modeled, that effect was deduced from the slowing down of the recovery, whereas the AO flux was still increasing (1987–1989 and 1998–2001 in Fig. 13, 1988–1989 in Fig. 14), which is especially visible by comparison with our constant yield model also displayed in these figures. It would be very interesting to build a more complex model involving many layers and a differential aging and polymerization of the layers. The general idea of using AO erosion as a probe to test the layer structure of a deposit is also interesting. Although many other diagnostics are already available on the ground, this method could also be ground tested, mostly to validate its use in space, where it is of simple and "automatic" use thanks to the strong AO density variations related to the solar cycle (at least at altitudes typical of SPOT, around 800 km).

When reaching such a refined analysis of the data and complexity of the mechanisms involved, the real character of the extra phenomena considered has to be assessed. In other words, are we not always adding extra parameters to the model to be able to fit the data, completely misunderstanding the physics? This is the danger of empirical models that was stated in the methodology section. We think not. First, from a qualitative standpoint, it is absolutely reasonable to assume that contaminants just deposited (physically adsorbed) are easier to "erode" than contaminants deposited three months before (chemically bonded through UV), which are easier to erode than contaminants deposited years before (higher reticulation). That was simply not used in this first model, which had to remain simple, but it is physically obvious. Second, from a quantitative standpoint, the values used for the erosion yields look reasonable. The Kapton erosion rate of $3 \times 10^{-24}$ cm$^3$/atom roughly means that approximately five oxygen atoms are necessary to "detach" one carbon atom or one methyl group (simple approximation considering only hydrocarbon). This is of course a crude view of what happens, because larger chains can also be eroded, but it gives an idea of the average erosion efficiency. From this, erosion rates 20 times larger than Kapton used here for newly deposited contaminant (just adsorbed) means that one oxygen atom is able to "extract" one propyl group from the adsorbed layers. It looks rather reasonable when the large energy that AO can supply (very reactive radical with an extra 5 ev of kinetic energy) is compared to the small adsorption energies (typically less than 1 eV). The erosion yields for "old" contaminants are also in a reasonable range. The value used was twice the Kapton yield, but we saw that a larger value was to be used for month-old contaminants (between 2 and 20), whereas a smaller value looked necessary to explain the nonerosion of year-old layers (around 0.1 Kapton or lower). These values are within a reasonable range, and are larger than the Teflon yield for the latter, in particular. The time scale for the polymerization and reticulation of contaminant at the origin of the reduced erosion yield is also reasonable. Figure 13 (and Fig. 14) shows that the big change happens for layers that are a few years old (typically 2 to 4), hence around 5 000 to 10,000 equivalent solar hours. This is close to typical time scales for contaminant UV darkening (Refs. 5, 10, and 11 and unpublished work at the ONERA Space Environment Department), which are indeed expected to be similar to fixation time scales because both phenomena are UV-induced through globally similar intermediate steps (electronic excitations, radical formations, ionizations).

#### Alternative Explanations

The mechanisms discussed make a very consistent picture, both from a physical standpoint and from a numerical point of view. However, any other possible explanation of the flight data must also be considered.

Indeed the first explanation considered to explain the flight data, before contamination, was that materials were degraded superficially and then cleaned superficially via AO erosion. However, this turned out not to be quantitatively consistent with the data. Recovery occurs for AO fluxes just above $10^{10}$ cm$^{-2}$s$^{-1}$, which are only able to erode a few angstroms of Teflon per year. This is much smaller than the penetration of any of the environment components that may degrade Teflon, such as UV, electrons, or protons.

The only environment component that might have such superficial effects is AO itself. The only possibility of having a really superficial degradation of Teflon would thus be if it originates from a synergy between radiations and AO as observed on the Long Duration Exposure Facility (LDEF),[5] but again this phenomenon looked inconsistent with the data. Invoking AO-radiation synergistic degradation of Teflon to explain SPOT data would require that 1) during solar minimum, radiations and little AO degrade the Teflon on SPOT; 2) during solar maximum, radiations and more AO clean the Teflon on SPOT by eroding superficial layers; and 3) on the LDEF, radiations and much more AO degrade the Teflon again. This unlikely nonmonotonous behavior of AO effects as a function of AO flux most certainly excludes this mechanism. The AO flux is probably too low at 800 km to contribute significantly to Teflon degradation, because this effect has only been noticed on the LDEF after a long time spent at a very low altitude.

The impossibility of identifying any other alternative mechanism, together with the quite accurate quantitative explanation through contamination, makes us confident in the correctness of the mechanisms reported in this paper.

## Conclusions

The evolution of the thermal behavior of SPOT spacecraft was explained qualitatively and quantitatively. It was shown to be mostly due to contamination. The cyclic succession of degradation and curing periods was caused by the cleaning of contamination by AO.

A thorough quantitative analysis showed that many features of the contamination and erosion rates were very naturally explained by UV exposure, whereas they remained unexplained without this extra environmental phenomenon. The leading-face degradation (and subsequent curing) is larger than that on other faces; it thus experiences a larger contamination deposition rate. The reason is that the contaminants condensed in eclipse become UV-fixed when the leading face is exposed to sunlight at eclipse exit, whereas on a sun-synchronous orbit the other faces are only exposed to UV later, after the spacecraft has already become warmer. The time evolution of the deposition rate on these ram faces is constant or hardly decreasing, which is another typical behavior of UV deposition. The third UV-related effect is the observation that the contaminant layers deposited for a long time are much harder to erode by AO, certainly because of a larger polymerization than the more recent superficial layers.

The operational consequences of these observations are twofold. First, the thermal coating aging due to contamination is significantly reduced by AO erosion. The erosion yield for the contaminant on SPOT spacecraft is rather important, probably larger than the reference Kapton erosion rate. It is, however, very dependent on the chemical nature of the contaminants, because AO definitively bonds silicones by turning them into silicates. The second operational information is the effect of UV for fixing contaminants through chemical bonding, even reducing their capability to be eroded by AO.

The simple model built for the SPOT spacecraft series thus accomplished the virtue of unraveling the physics involved. It proved some predictive character for similar spacecraft (from SPOT 1 to SPOT 2) but it could not provide any predictions for a different spacecraft. A predictive assessment of contamination effects on a different spacecraft would indeed require two extra experiments. First, an identification of the contaminant sources and a physical computation of the transport should be performed at spacecraft level. Second, a sophisticated physical model of the UV-induced fixation and aging should be built. It should, in particular, be able to deal with nonstationary situations due to the thermal cycling and the sunlight onset at eclipse exit. Whereas contamination transport models exist, only a steady-state model of UV-enhanced depositions adapted to GEO conditions is available.[9] We are thus in the process of building such a nonsteady model based on theoretical analysis, SPOT data, and ongoing ground experiments.

## References

[1] Alet, I., "Two Years of In-Orbit Life of SPOT 1 Heliosynchronous Platform," *3rd European Symposium on Space Thermal Control & Life Support Systems*, SP-288, ESA, Noordwijk, The Netherlands, 1988, pp. 423, 427, 950.

[2] Alet, I., "SPOT Multimission Platform Thermal Control—Five Years of In-Flight Results," *4th European Symposium on Space Environmental and Control Systems*, SP-324, ESA, Florence, Italy, 1991, pp. 945–950.

[3] Alet, I., "Eleven Years of Ageing of SSM Teflon on the Sunsynchronous Orbit—SPOT," *7th International Symposium on Materials in Space Environment*, SP-399, ESA, Toulouse, France, 1997, pp. 283–286.

[4] Anderson, B. J. (ed.), "Natural Orbital Environment Definition Guidelines for Use in Aerospace Vehicle Development," NASA TM-4527, N94-36175, June 1994.

[5] Silverman, E. M., "Space Environment Effects on Spacecraft: LEO Materials Selection Guide," NASA CR 4661, Aug. 1995.

[6] Koontz, S., Leger, L., Albyn, K., and Cross, J., "Vacuum Ultraviolet Radiation/Atomic Oxygen Synergism in Material Reactivity," *Journal of Spacecraft and Rockets*, Vol. 27, No. 3, 1990, pp. 346–348.

[7] Hall, D. F., and Fote, A. A., "Thermal Control Coatings Performance at Near Geosynchronous Orbit," *Journal of Thermophysics and Heat Transfer*, Vol. 6, No 4, 1992, pp. 665–671.

[8] Tribble, A. C., and Haffner, J. W., "Estimates of Photochemically Deposited Contamination on the GPS Satellites," *Journal of Spacecraft*, Vol. 28, No. 2, 1991, pp. 222–228.

[9] Stewart, T. B., Arnold, G. S., Hall, D. F., and Marten, H. D., "Absolute Rates of Vacuum-Ultraviolet Photochemical Deposition of Organic Films," *Journal of Physical Chemistry*, Vol. 93, March 1989, pp. 2393–2400.

[10] Alred, J. W., and Soares, C., "Solar Absorptivity as a Function of Spacecraft External Contamination," *33rd International SAMPE Technical Conference "Advancing Affordable Materials Technology,"* Society for the Advancement of Material and Process Engineering, Covina, CA, Nov. 2001.

[11] Stewart, T. B., Arnold, G. S., Hall, D. F., Marvin, D. C., Hwang, W. C., Young Owl, R. C., and Marten, H. D., "Photochemical Spacecraft Self-Contamination: Laboratory Results and System Impacts," *Journal of Spacecraft and Rockets*, Vol. 26, No. 5, 1989, pp. 358–367.

N. Gatsonis
*Associate Editor*